Accepted Article

Title: Effect of Cp-Ligand Methylation on Rh(III)-Catalyzed Annulations of Aromatic Carboxylic Acids with Alkynes: Synthesis of Isocoumarins and PAHs for Organic Light-Emitting Devices

Authors: Alexander P. Molotkov, Mikhail A. Arsenov, Daniil A. Kapustin, Dmitry V. Muratov, Nikolay E. Shepel', Yury V. Fedorov, Alexander F. Smol'yakov, Elena I. Knyazeva, Dmitry A. Lypenko, Artem V. Dmitriev, Alexey E. Aleksandrov, Eugeny I. Maltsev, and Dmitry Loginov

This manuscript has been accepted after peer review and appears as an Accepted Article online prior to editing, proofing, and formal publication of the final Version of Record (VoR). This work is currently citable by using the Digital Object Identifier (DOI) given below. The VoR will be published online in Early View as soon as possible and may be different to this Accepted Article as a result of editing. Readers should obtain the VoR from the journal website shown below when it is published to ensure accuracy of information. The authors are responsible for the content of this Accepted Article.

Effect of Cp-Ligand Methylation on Rh(III)-Catalyzed Annulations of Aromatic Carboxylic Acids with Alkynes: Synthesis of Isocoumarins and PAHs for Organic Light-Emitting Devices

Alexander P. Molotkov,[a] Mikhail A. Arsenov,[a] Daniil A. Kapustin,[a] Dmitry V. Muratov,[a] Nikolay E. Shepel',[a] Yury V. Fedorov,[a] Alexander F. Smol'yakov,[a,b,c] Elena I. Knyazeva,[b] Dmitry A. Lypenko,[d] Artem V. Dmitriev,[d] Alexey E. Aleksandrov,[d] Eugeny I. Maltsev,[d] Dmitry A. Loginov*[a]

Abstract

An efficient protocol for the synthesis of π-extended isocoumarins and polycyclic aromatic hydrocarbons based on the oxidative coupling of aromatic carboxylic acids with internal alkynes catalyzed by (cyclopentadienyl)rhodium complexes was developed. The chemoselectivity strongly depends on the methylation of the Cp ligand. The pentamethyl derivative $[Cp*RhCl_2]_2$ predominantly gives isocoumarin moiety, while the non-methylated complex $[CpRhI_2]_n$ results in naphthalene derivatives. The polyaromatic carboxylic acids (such as 1-naphthoic acid, 1-pyrenecarboxylic acid, fluorene-1-carboxylic acid, and dibenzofuran-4-carboxylic acid) are suitable for this approach. A mixture of $Cp*H/RhCl_3$ can be used as a catalyst instead of $[Cp*RhCl_2]_2$. The structures of 3,4-diphenylindeno[1,2-h]isochromen-1(11H)-one and 7,10-dimethyl-8,9-diphenylbenzo[pqr]tetraphene were determined by X-ray diffraction. The optical properties of the compounds prepared were studied. 7,8-Diphenyl-10H-phenaleno[1,9-gh]isochromen-10-one was employed as an emissive layer for OLED manufacturing. The OLED emits yellow-green light of maximum intensity 1740 cd·m^{-2} at 15 V.

[a] A. P. Molotkov, M. A. Arsenov, D. A. Kapustin, Dr. D. V. Muratov, Dr. N. E. Shepel', Prof. Dr. Y. V. Fedorov, Dr. A. F. Smol'yakov, Prof. Dr. D. A. Loginov
A. N. Nesmeyanov Institute of Organoelement Compounds, Russian Academy of Science, 28 ul. Vavilova, 119991 Moscow, Russian Federation
E-Mail: dloginov@ineos.ac.ru
Homepage: http://www.ineos.ac.ru/en
[b] Dr. A. F. Smol'yakov, E. I. Knyazeva
Faculty of Science, RUDN University, 6 Miklukho-Maklaya St., Moscow 117198, Russian Federation
[c] Dr. A. F. Smol'yakov
Plekhanov Russian University of Economics, Stremyanny per. 36, Moscow, 117997, Russian Federation
[d] Dr. D. A. Lypenko, Dr. A. V. Dmitriev, A. E. Aleksandrov, Prof. Dr. E. I. Maltsev
A.N. Frumkin Institute of Physical Chemistry and Electrochemistry of the Russian Academy of Sciences, Leninsky Prosp. 31, bld.4, Moscow 119071, Russian Federation

Introduction

In the last few decades, organic light-emitting diodes (OLEDs) have attracted much attention from chemists and material scientists due to their wide application in light sources and flat-panel color.[1] Tang and VanSlyke pioneered OLED technology.[2] In 1987, they constructed the first organic light-emitting diode using 8-hydroxyquinoline aluminum as an emissive layer. Isocoumarins, as well as polycyclic aromatic hydrocarbons (PAHs), are of special interest due to their high stability and fluorescent properties. In particular, these compounds have a flat π-conjugated structure, which provides a strong increase in the Stokes shift of fluorescence emission.[3] It was shown that tetracene and pyrene derivatives can be used for the OLED construction as transport and emitting layers.[4]

Transition metal catalyzed organic reactions are a promising approach for the construction of isocoumarins and PAHs. For example, various palladium-catalyzed intra- and intermolecular cyclization reactions of halogen-substituted benzene derivatives have been well established as one of the most efficient strategies for the synthesis of isocoumarins.[5] In a similar manner, it was found that the coupling of aryl iodides with alkynes can be used for the construction of a naphthalene moiety.[6] Arylboronic acids, triarylmethanols, and aroyl chlorides were also successfully introduced into this reaction using rhodium and iridium catalysis.[7] But the main disadvantage of these protocols is the low atom economy due to a large amount of waste. At the same time, straightforward C–H activation reactions usually require the presence of directing groups (e.g. pyrazole and ketone functions) to provide selectivity.[8] Cramer with co-workers reported the synthesis of various naphthalene and anthracene derivatives via C–H functionalization without any leaving and directing groups.[9] However, it should be noted that this protocol allows to selectively obtain only products with a linear structure.

The oxidative coupling of aromatic carboxylic acids with internal alkynes via C–H activation is of particular interest due to the great step and atom economy of this method, as well as the possibility to synthesize both isocoumarins and PAHs.[10] The reaction proceeds through the chelation-assistance of the carboxylic group, which provides the selectivity of C–H activation in the *ortho* position.[11] Satoh and Miura were pioneers in the development of this strategy.[12] In particular, they showed that the pentamethylcyclopentadienyl complex [Cp*RhCl$_2$]$_2$ effectively catalyzes the coupling of benzoic acids with internal alkynes in the presence of Cu(OAc)$_2$ as an oxidant, predominantly giving isocoumarins with a side formation of naphthalenes (3–14%).[13] The latter products are formed as a result of decarboxylation. In contrast, we found that the non-methylated complex [CpRhI$_2$]$_n$ in the same reaction selectively gives only naphthalene derivatives.[14] Shibata and Tanaka with co-workers showed that the oxidant nature (Cu(II) or Ag(I)) also have a crucial impact on the selectivity in the case of usage of electron-deficient

2

rhodium complex [Cp′RhCl$_2$]$_2$ (Cp = 1,3-(COOEt)$_2$-C$_5$Me$_3$) as a catalyst.[15] In the last decade, efficient catalytic systems with different selectivity based on other transition metal complexes have been also developed.[16,17]

Herein we report on the use of the rhodium complexes [Cp*RhCl$_2$]$_2$ and [CpRhI$_2$]$_n$ for the synthesis of π-extended isocoumarins and PAHs using various polyaromatic carboxylic acids (e.g. 1-naphthoic acid, 1-pyrenecarboxylic acid, fluorene-1-carboxylic acid, etc.) as coupling partners. Moreover, we investigated the fluorescent properties of the compounds prepared and used them for the OLED manufacturing.

Results and Discussion

The general procedure for the synthesis of isocoumarins and PAHs is given in Table 1. The complexes [Cp*RhCl$_2$]$_2$ and [CpRhI$_2$]$_n$ were chosen as catalysts, because they are easily available in comparison with other known catalytic systems. Thus, the non-methylated complex [CpRhI$_2$]$_n$ can be easily synthesized by a two-step procedure based on the reaction of [(cod)RhCl]$_2$ (cod = 1,5-cyclooctadiene) with CpTl followed by treatment of the resulting CpRh(cod) by iodine in a total yield of 97%,[18] while the methylated derivative [Cp*RhCl$_2$]$_2$ is prepared by direct interaction of rhodium chloride with C$_5$Me$_5$H.[19] As can be seen from Table 1, in the case of benzoic acid and its derivatives, the selectivity of the reaction strongly depends on the methylation of the Cp ligand in the catalyst (Table 1, Entries 1–7), predominantly giving isocoumarins for [Cp*RhCl$_2$]$_2$ and naphthalene derivatives for [CpRhI$_2$]$_n$. The reaction is tolerant to the functional groups Cl and MeO in the aromatic ring. At the same time, the presence of the NO$_2$-group significantly reduces the yields of the desired products (Table 1, Entry 7). Diphenyl-, diethyl- and bis(*p*-methoxyphenyl)acetylenes as well as 1-phenyl-1-propyne are suitable for the reaction. However, attempts to perform oxidative coupling of benzoic acid with 1,4-dimethoxy-2-butyne, bis(trimethylsilyl)acetylene or phenylacetylene have failed.

The developed synthetic protocols have been successfully extended to polyaromatic carboxylic acids, such as 1-naphthoic, fluorene-1-carboxylic, dibenzofuran-4-carboxylic and 1-pyrenecarboxylic acids (Table 1, Entries 8–16). It is interesting to note that although the complex [Cp*RhCl$_2$]$_2$ usually leads to isocoumarins, the catalyzed reaction of dibenzofuran-4-carboxylic acid with diphenylacetylene affords naphthalene **2l** as a sole product (Table 1, Entry 12). Similarly, the replacement of diphenylacetylene by diethylacetylene in coupling with fluorene-1-carboxylic acid catalyzed by [CpRhI$_2$]$_2$ results in the formation of isocoumarin **1k** instead of the expected naphthalene derivative (Table 1, Entry 11 *vs* 9). The low selectivity of the [Cp*RhCl$_2$]$_2$-catalyzed reaction of 1-pyrenecarboxylic acid with diphenylacetylene is an additional exception to the general tendency (Table 1, Entry 13). The observed non-selectivity

3

may be explained by changes of the oxidation potentials of the reaction intermediates as a result of the influence of different functional groups.[16d,20] It should be noted that the oxidation potentials depend not only on the nature of the carboxylic acid but also on the electronic properties of the incoming alkyne and the supporting ligand at the rhodium atom. The key possible intermediate **A** is presented on Scheme 1. When the redox potential of the Cu(II)/Cu(I) couple is sufficient for the oxidation of **A**, the reaction proceeds via the reductive elimination of rhodium to give the isocoumarin product. Otherwise, the decarboxylation is more favorable and leads to the naphthalene derivatives after insertion of the second alkyne molecule.
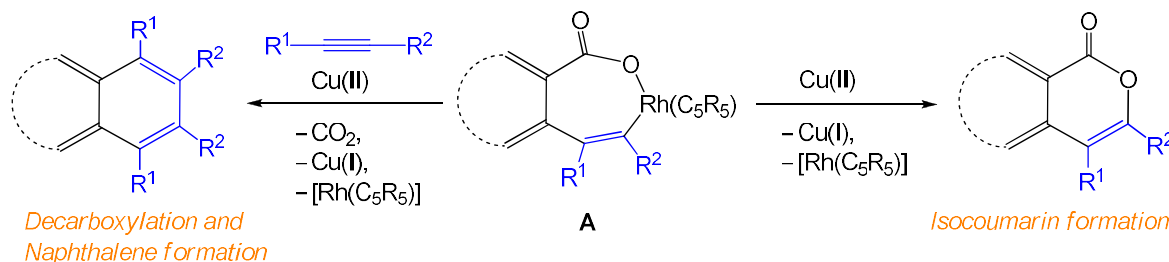
Scheme 1. The key intermediate **A** and possible reaction pathways for the oxidative coupling of aromatic carboxylic acids with internal alkynes.

The ^{1}H NMR spectra of isocoumarins **1a–e**, **1h–i**, **1k**, **1m**, and **1n** display strongly down-field shifted doublet at more than 8.00 ppm. In contrast, the phenyl-substituted naphthalene derivatives **2a**, **2d–g**, **2i**, **2j**, **2l**, **2m**, and **2o** show a characteristic multiplet signal in the range of 6.8–7.1 ppm, thus making ^{1}H NMR spectroscopy sufficiently informative to monitor the reaction selectivity. The structures of **1i** and **2o** were confirmed by single-crystal X-ray diffraction study (Fig. 1 and 2).[21] The polyaromatic moiety is ca. planar for both compounds, being slightly twisted in the case of benzopyrene derivative **2o**. The phenyl substituents are not coplanar with a polyaromatic moiety (dihedral angles are 27.5º and 80.2º for **1i**; 70.5º and 77.6º for **2o**).
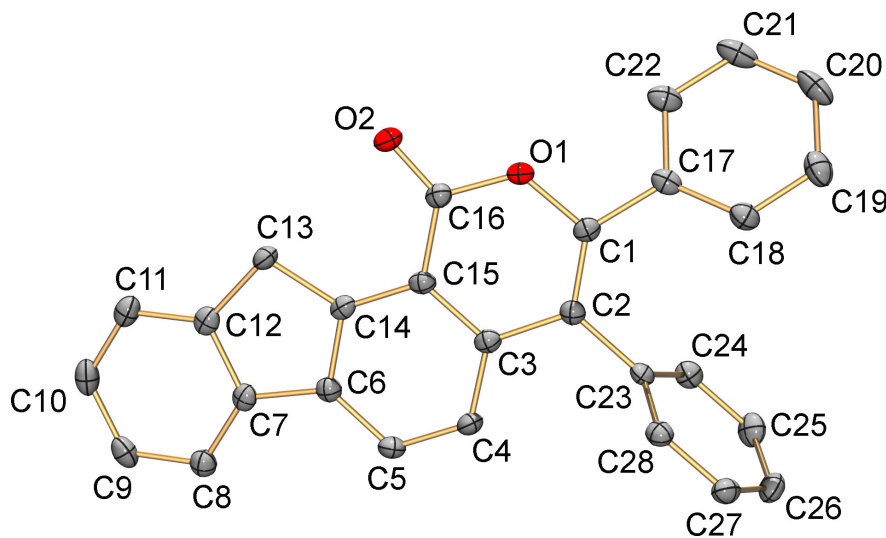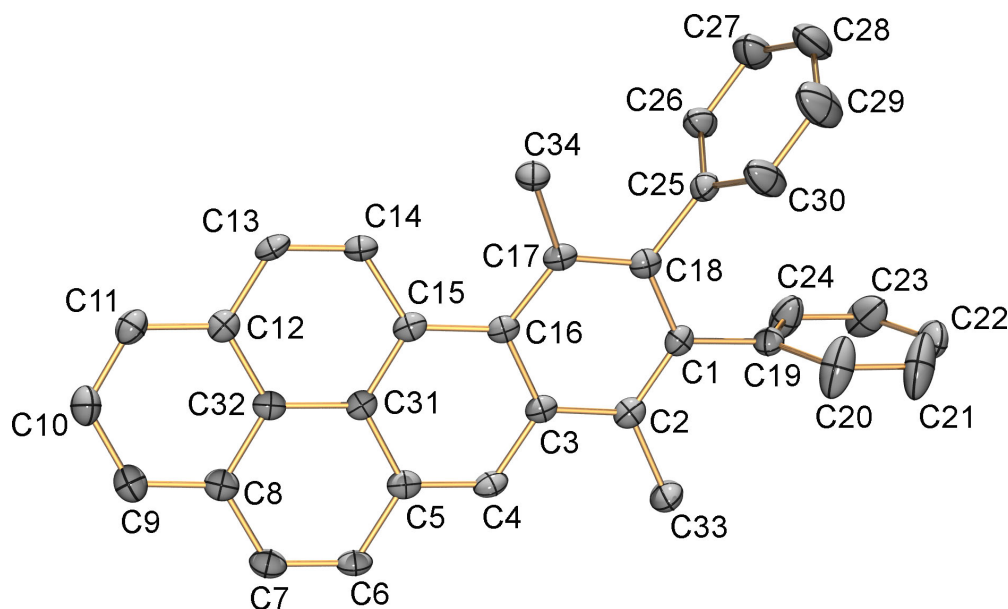

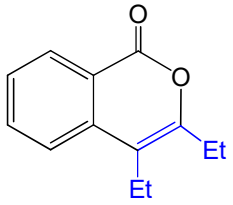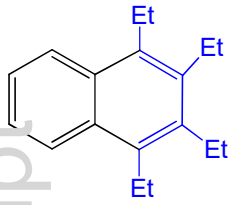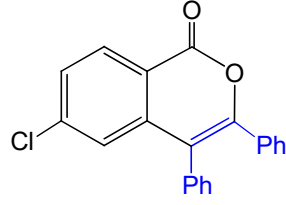**Figure 1**. X-Ray diffraction structure of compound **1i**. Hydrogen atoms are omitted for clarity.
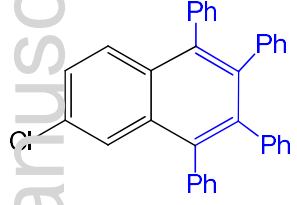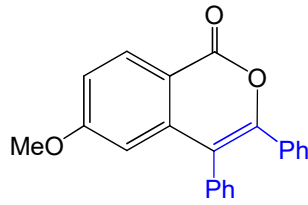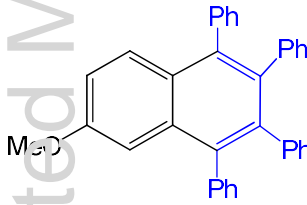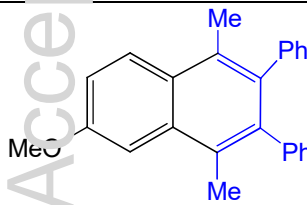
4

Figure 2. X-Ray diffraction structure of compound **2o**. Hydrogen atoms are omitted for clarity.
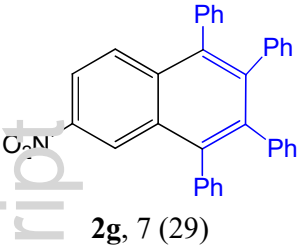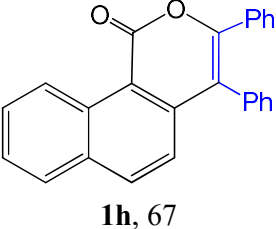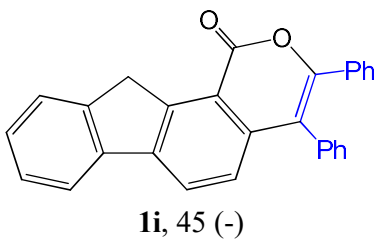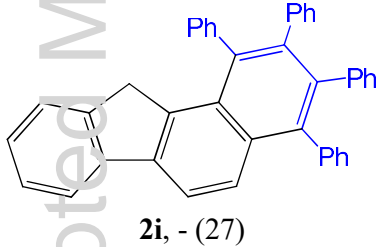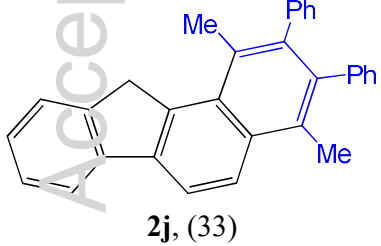
To simplify the reaction procedure, we tested mixtures of RhCl$_3$ with various cyclopentadienes as catalytic systems (Table 2).[22] As a model reaction, we chose the oxidative coupling of benzoic acid with diphenylacetylene. It was found that a mixture of RhCl$_3$ with C$_5$Me$_5$H (Table 2, Entry 1) has the same selectivity and catalytic activity as the complex [Cp*RhCl$_2$]$_2$ (Table 1, Entry 1), giving predominantly isocoumarin **1a**. Unexpectedly, the use of non-methylated cyclopentadiene C$_5$H$_6$ did not give any organic products (Table 2, Entry 4). In a similar manner, methyl- and tetramethylcyclopentadienes proved to be inefficient as additives to RhCl$_3$ in this reaction (Table 2, Entries 2 and 3). At the same time, rhodium chloride without any supporting ligands gives naphthalene **2a** in 31% yield (Table 2, Entry 5), suggesting that the presence of cyclopentadienes less substituted than C$_5$Me$_5$H can poison the catalyst. It may be explained by the formation of inactive rhodium compounds, for example, rhodocenium cations.

5
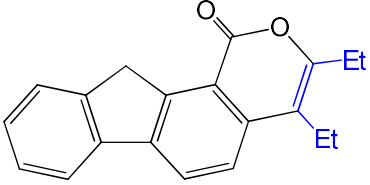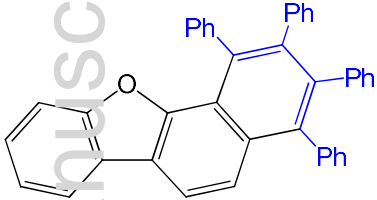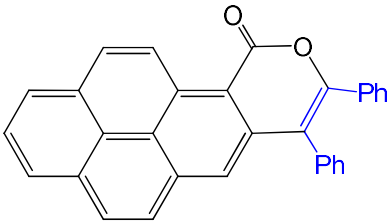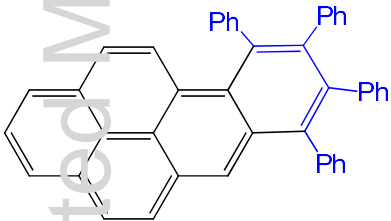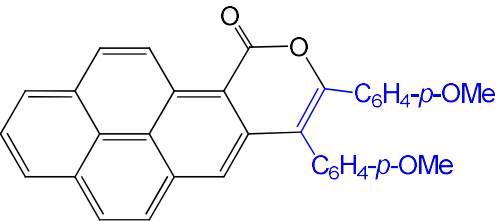
Table 1. The reaction of aromatic carboxylic acids with internal alkynes.[a]
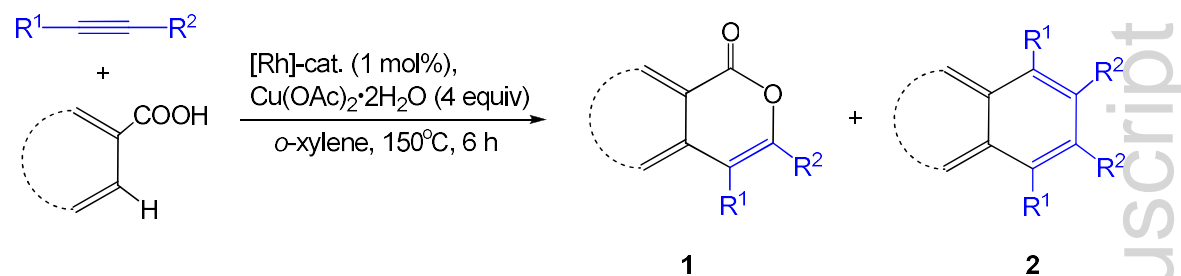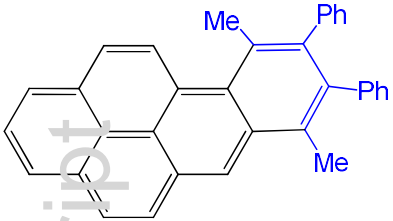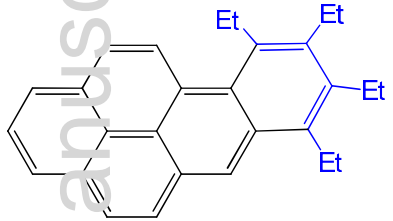
Entry	Acid	R^1, R^2	Isocoumarin product, yield [%][b]	Naphthalene product, yield [%][b]
1	Benzoic acid	Ph, Ph	**1a**, 51 (-)	**2a**, 2 (91)
2	Benzoic acid	p-MeOC$_6$H$_4$, p-MeOC$_6$H$_4$	**1b**, 56 (12)	**2b**, 4 (66)

6

3	Benzoic acid	Et, Et	**1c**, 88 (-)	**2c**, - (69)
4	4-Chlorobenzoic acid	Ph, Ph	**1d**, 52 (2)	**2d**, - (52)
5	4-Methoxybenzoic acid	Ph, Ph	**1e**, 53 (-)	**2e**, - (69)
6	4-Methoxybenzoic acid	Me, Ph	-	**2f**, (40)

7	4-Nitrobenzoic acid	Ph, Ph	-	**2g**, 7 (29)
8	1-Naphthoic acid	Ph, Ph	**1h**, 67	-
9	Fluorene-1-carboxylic acid	Ph, Ph	**1i**, 45 (-)	**2i**, - (27)
10	Fluorene-1-carboxylic acid	Me, Ph	-	**2j**, (33)

8

11	Fluorene-1-carboxylic acid	Et, Et	 **1k**, (15)	-
12	Dibenzofuran-4-carboxylic acid	Ph, Ph	-	 **2l**, 57
13	1-Pyrenecarboxylic acid	Ph, Ph	 **1m**, 29 (-)	 **2m**, 36 (52)
14	1-Pyrenecarboxylic acid	*p*-MeOC₆H₄, *p*-MeOC₆H₄	 **1n**, 62	-

9

| 15 | 1-Pyrenecarboxylic acid | Me, Ph | - | **2o**, (73) |
| 16 | 1-Pyrenecarboxylic acid | Et, Et | - | **2p**, (55) |

[a] Reaction conditions: acid (0.50 mmol), alkyne (1.00 mmol), [Cp*RhCl$_2$]$_2$ (1 mol% of Rh, 0.0025 mmol), Cu(OAc)$_2$·2H$_2$O (4 equiv, 2.00 mmol) in *o*-xylene, heating at 150ºC for 6 h, see general procedure. [b] Yields are given for isolated products. Values in parentheses indicate yields when [CpRhI$_2$]$_n$ was used as a catalyst. .

10

Table 2. The oxidative coupling of benzoic acid with diphenylacetylene catalyzed by mixtures of RhCl$_3$ with cyclopentadienes.[a]

Entry	Cyclopentadiene	**1a**, yield [%][b]	**2a**, yield [%][b]
1	C$_5$Me$_5$H	84	7
2	C$_5$HMe$_4$H	5	-
3	C$_5$H$_4$MeH	-	-
4	C$_5$H$_6$	-	-
5	None	-	31

[a] Reaction conditions: benzoic acid (0.50 mmol), diphenylacetylene (1.12 mmol), RhCl$_3$ (2 mol%, 0.01 mmol), cyclopentadiene (12 mol%, 0.06 mmol), Cu(OAc)$_2$·2H$_2$O (4 equiv, 2.00 mmol) in o-xylene, heating at 150 ºC for 6 h. [b] Yields are given for isolated products.

Photophysical Properties

Absorption and fluorescence spectra in CH$_3$CN were measured to study the optical properties of the prepared compounds (Table 3). Both isocoumarins and naphthalenes showed fluorescence emission in the blue-green region (Fig. 3). For example, the absorption spectrum of compound **2m** demonstrates a set of absorption bands with different intensities. The most broad and intense are one at 310 nm, a doublet of bands at 280 nm, several bands at 239, 382 and 401 nm (Fig. 4). There are several low-intensity bands that are responsible for the formation of the shoulder in the absorption spectrum. To make spectral assignments, we calculated the electronic absorption spectra for the most representative compounds (**1m** and **2m**) using the TD-DFT method. This method has earlier proven its usefulness for prediction of UV–Visible spectra of organic dyes.[23] First of all, we tested various exchange–correlation functionals (B3LYP, CAM-B3LYP, and PBE0) to compare the results of the energy gaps with the experimentally obtained data (Table 4). In accordance with the general trend,[23] the best correlations were obtained for the B3LYP and PBE0 functionals. The CAM-B3LYP functional overestimates the differences in energy between the frontier orbitals. The lowest energy bands for both compounds mainly derive from HOMO → LUMO orbitals, which correspond to the π → π* transitions. These frontier orbitals are located on the pyrene moiety (for details, see Supporting Information). It is

11

interesting to note that the most intensive band for the isocoumarin compound **1m** (310 nm) involves the HOMO–2 → LUMO transition, which corresponds to charge transfer from phenyl substituents to the pyrene moiety because the HOMO–2 orbital is located on the phenyl groups. In the case of the naphthalene compound **2m**, the high energy bands are formed by several transitions and are difficult for interpretation.

The emission spectrum of **2m** consists of two evident maxima, but a shoulder of about 500 nm indicates the existence of another maximum. Three Gauss curves fit yields 3 maxima at 426, 447 and 458 nm (Fig. 5).
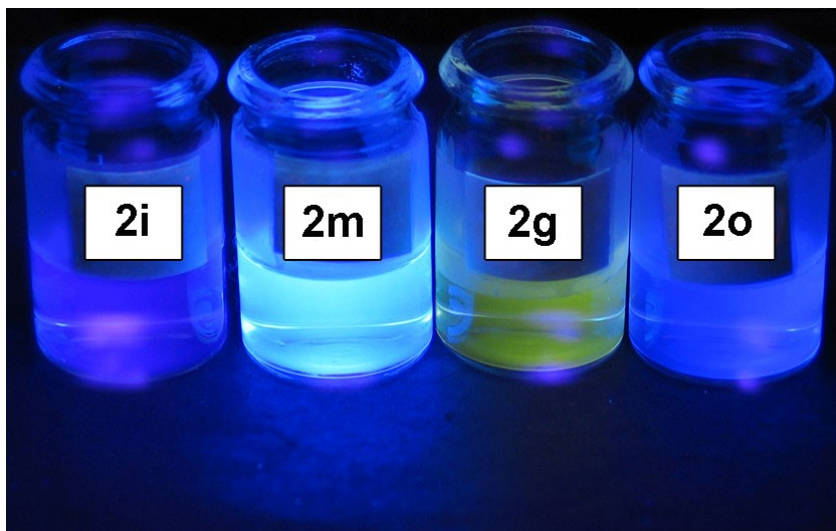
Figure 3. The photo of acetonitrile solutions of **2g**, **2i**, **2m** and **2o** exposed to UV light (365 nm).
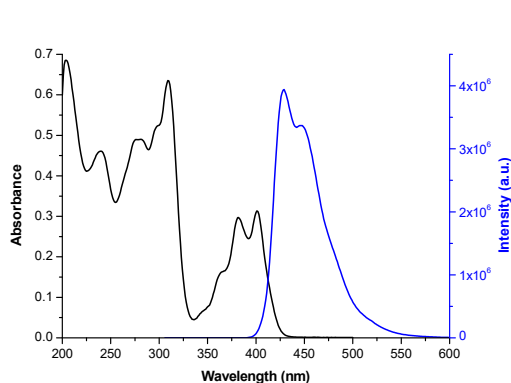
Figure 4. The absorption spectrum of **2m** in $CH_3CN+CH_2Cl_2$ (<1.0%), C = $2 \cdot 10^{-5}$ M, L=1 cm and emission spectrum of **2m** in $CH_3CN+CH_2Cl_2$ (<0.2%), C = $3.3 \cdot 10^{-6}$ M, λ_{ex} = 382 nm, 20 °C.
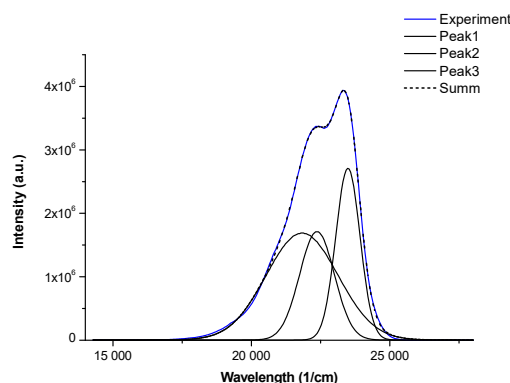
Figure 5. Gauss curves approximation of the emission spectrum of compound **2m**: experimental and mathematical approximation: by component and summarized (fully consistent with experimental).

We found that for both isocoumarin and naphthalene derivatives the additional π-conjugation as well as the introduction of donor substituents (Cl and OMe) at position 6 of 3,4-diphenylisocoumarin (**1a**) and 1,2,3,4-tetraphenylnaphthalene (**2a**) leads to a slightly

12

hypsochromic shift of the fluorescence emission (Table 3, Entries 3–6 and 8 *vs* 1, as well as Entries 11–14 and 8 *vs* 9). In contrast, the introduction of a strong acceptor nitro group at position 6 of **2a** results in a bathochromic shift (Entry 10 *vs* 9). In the case of benzopyrene compounds **2m**, **2o** and **2p** the maxima of fluorescent emission only slightly depend on the number of phenyl substituents (Entries 12–14).

Using the optimal excitation wavelength, the obtained luminescence spectra were used to calculate the quantum yields (see Table 3). Surprisingly, isocoumarin derivatives showed low quantum yields. In most cases except for the pyrene compound **1m** (Table 3, Entries 8 *vs* 1–7) their values are below 1%. Moreover, the replacement of phenyl substituents with ethyl groups did not improve the fluorescence efficiency (Entry 2). In contrast, naphthalenes have rather high quantum yields (Entries 11–14), which are comparable with quinine sulfate.

The absorption and fluorescence spectra for compounds **1m** and **2m** were also recorded in dichloromethane, acetone, dimethylsulfoxide, and ethanol (see the Supporting Information). No significant solvatochromic effects were observed. In particular, the maximum shifts of absorption and emission bands are 6 and 12 nm, respectively, being smaller for the naphthalene compound **2m** (Table 5).

Table 3. Optical properties of compounds **1a,c,d,e,h,i,k,m** and **2a,g,l,m,o,p**.

Entry	Compound	Significant absorption maxima, extinction coefficients ε (λ_{max}, [nm]), [L×mol^{-1}×cm^{-1}]	Emission bands maxima, [nm]	Emission quantum yields φ (λ_{ex}, [nm])
1	**1a**	$\varepsilon_{295} = 14\ 865$, $\varepsilon_{334} = 7\ 261$, $\varepsilon_{227} = 25\ 455$	481 [a]	0.1% (330)
2	**1c**	$\varepsilon_{269} = 7\ 290$, $\varepsilon_{279} = 6\ 160$, $\varepsilon_{260} = 5\ 950$, $\varepsilon_{328} = 2\ 830$[c]	403	0.4% (328)
3	**1d**	$\varepsilon_{300} = 13\ 462$, $\varepsilon_{338} = 6\ 025$, $\varepsilon_{239} = 26\ 676$	468 [a]	0.2% (327)
4	**1e**	$\varepsilon_{259} = 34\ 358$, $\varepsilon_{304} = 11\ 548$	406 [a]	<0.1% (315)
5	**1h**	$\varepsilon_{285} = 30\ 885$, $\varepsilon_{242} = 25\ 197$, $\varepsilon_{369} = 10\ 846$, $\varepsilon_{385} = 7\ 544$	440 [a]	<0.1% (330)
6	**1i**	$\varepsilon_{315} = 18\ 468$, $\varepsilon_{363} = 12\ 433$, $\varepsilon_{253} = 13\ 290$	451, 420, 399 [b]	0.4% (315)
7	**1k**	$\varepsilon_{310} = 17\ 000$, $\varepsilon_{298} = 17\ 500$, $\varepsilon_{357} = 6\ 100$[c]	391, 411, 434 [b]	4.2% (355)
8	**1m**	$\varepsilon_{310} = 41\ 490$, $\varepsilon_{373} = 21\ 147$, $\varepsilon_{355} = 13\ 836$, $\varepsilon_{411} = 7\ 325$, $\varepsilon_{433} = 8\ 680$	502, 472, 447 [b]	9.2% (355) [d] 2.7% (365) [e]
9	**2a**	$\varepsilon_{294} = 11\ 072$, $\varepsilon_{239} = 45\ 956$	467 [a]	-
10	**2g**	$\varepsilon_{277} = 21\ 433$; $\varepsilon_{323} = 6\ 244$; $\varepsilon_{375} = 2\ 925$	550	1.4% (380)

13

11	**2l**	$\varepsilon_{269} = 65\ 642$; $\varepsilon_{292} = 31\ 559$; $\varepsilon_{333} = 7\ 872$; $\varepsilon_{351} = 6\ 234$	360, 375, 390 [b]	25.5% (335)
12	**2m**	$\varepsilon_{310} = 31\ 715$; $\varepsilon_{280} = 24\ 493$ [c]; $\varepsilon_{239} = 23\ 033$, $\varepsilon_{382} = 14\ 862$; $\varepsilon_{401} = 15\ 665$	426, 447, 458 [b]	39.5% (382)
13	**2o**	$\varepsilon_{259} = 34\ 713$; $\varepsilon_{273} = 30\ 537$; $\varepsilon_{296} = 27\ 033$; $\varepsilon_{308} = 34\ 523$; $\varepsilon_{332} = 12\ 240$; $\varepsilon_{348} = 18\ 662$; $\varepsilon_{364} = 7\ 188$; $\varepsilon_{383} = 12\ 232$; $\varepsilon_{405} = 12\ 512$	451, 444, 421 [b]	31.2% (364)
14	**2p**	$\varepsilon_{307} = 35\ 000$; $\varepsilon_{295} = 26\ 700$; $\varepsilon_{272} = 28\ 400$, $\varepsilon_{261} = 24\ 200$; $\varepsilon_{385} = 13\ 800$, $\varepsilon_{406} = 14\ 500$	422, 441, 462 [b]	37.8% (383)

[a] Emission maxima are not well-defined due to low intensity. [b] All wavelength maxima are obtained from Gauss curves consistent with the emission spectrum. [c] A doublet of bands. [d] Fluorescence lifetime is equal to 1.58 ± 0.01 ns. [e] In solid state.

Table 4. The most intensive absorption bands for compounds **1m** and **2m** calculated at the B3LYP/DZP, CAM-B3LYP/DZP and PBE0/DZP levels.

Compound	Experimental λ_{max}, [nm]	Calculated λ_{max}, [nm]		
		B3LYP/DZP	CAM-B3LYP/DZP	PBE0/DZP
1m	433	403	348	392
	373	365	326	356
	310	305	273	303
2m	401	412	354	406
	310	327	272	323
	280	310	266	303

Table 5. The long-wavelength absorption and emission bands for compounds **1m** and **2m** in different solvents.

| Solvent	Absorption maxima, [nm]		Emission maxima, [nm]	
	1m	**2m**	**1m**	**2m**
Dichloromethane	376, 414, 437	313, 386, 405	450, 475, 490	423, 452, 462
Acetone	374, 412, 435	383, 403	447, 471, 500	428, 450, 460
Ethanol	376, 414, 437	310, 383, 402	449, 475, 492	428, 451, 459
Acetonitrile	373, 411, 434	309, 382, 402	447, 471, 501	427, 449, 458
Dimethylsulfoxide	379, 416, 438	313, 387, 406	452, 475, 502	430, 452, 467

OLED construction

14

To investigate the electron transport properties of the compounds prepared, we explored the possibility of making films on a glass substrate using the thermal vacuum evaporation procedure for **1a**, **1d**, **1e**, **1h**, **1m**, and **2l**. In the case of isocoumarins **1a** and **1e**, we failed to obtain films of the required quality due to crystallization during deposition or complete/partial decomposition of substances upon heating. For example, compound **1a** displayed an uneven regime of sublimation at 220–230 °C in a vacuum. The deposition rate varied within a wide range (0.1–1.0 Å·s^{-1}), so the layer of the required quality was not prepared. In the case of **1e**, the sublimation temperature was about 90 °C, and the deposition rate was 0.2–0.5 Å·s^{-1}. The obtained film turned out to be polycrystalline (matte) and, therefore, is not suitable for electron transport measurements. Finally, transparent films on glass substrates without visible indication of crystallization and discoloration were obtained for compounds **1m** and **2l** upon sublimation at 160 and 144 °C, respectively. Accordingly to thermogravimetric analysis (see the Supporting Information), compound **1m** is stable in the air till 300 °C. Although **1d** and **1h** gave matte films, we still managed to obtain the charge carrier mobility values for them. To measure the mobility of electrons and holes in the studied materials by means of the photo-MIS-CELIV method[24] the following structures were manufactured: glass/ ITO/ SiO$_2$ (70 nm)/ **1d**, **1h**, **1m**, or **2l** (100 nm)/ Al (100 nm) (Fig. 6a). The results are given in Table 6. We found that the mobility values lie in the range of 10^{-6}–10^{-5} cm^2·V^{-1}·s^{-1}, which is significantly lower than for materials usually used as transport layers (10^{-4}–10^{-2} cm^2·V^{-1}·s^{-1}). Therefore, these compounds cannot be applied as transport materials. Nevertheless, we used isocoumarin **1m** as an emissive layer in the OLED of the following structure (Fig. 6b): ITO/ TAPC (80nm) / **1m** (10nm)/ 3TRYMB (30nm)/ LiF (1nm)/ Al (100nm), where ITO is the anode, TAPC is the hole transporting layer, 3TRYMB is the electron transport layer, LiF/Al is the cathode. This OLED structure emits yellow-green light of maximum brightness 1740 cd·m^{-2} at 15 V (Fig. 7 and 8). The luminescence spectrum of isocoumarin **1m** in the solid state is represented in the Supporting Information for comparison.

Table 6. The electron and hole mobility, as well as conditions of the film formation for compounds **1d**, **1h**, **1m**, and **2l**.

Compound	Electron mobility, cm^2·V^{-1}·s^{-1}	Hole mobility, cm^2·V^{-1}·s^{-1}	Vacuum deposition temperature, °C	Vacuum deposition rate, Å·s^{-1}	Film quality
1d	$1.8 \cdot 10^{-5}$	$1.0 \cdot 10^{-5}$	110	0.1	Matte
1h	$5.75 \cdot 10^{-6}$	$5.84 \cdot 10^{-6}$	120	0.2	Matte
1m	$1.31 \cdot 10^{-5}$	$1.51 \cdot 10^{-4}$	160	0.26	Transparent
2l	$2.26 \cdot 10^{-6}$	$7.63 \cdot 10^{-6}$	144	0.15	Transparent
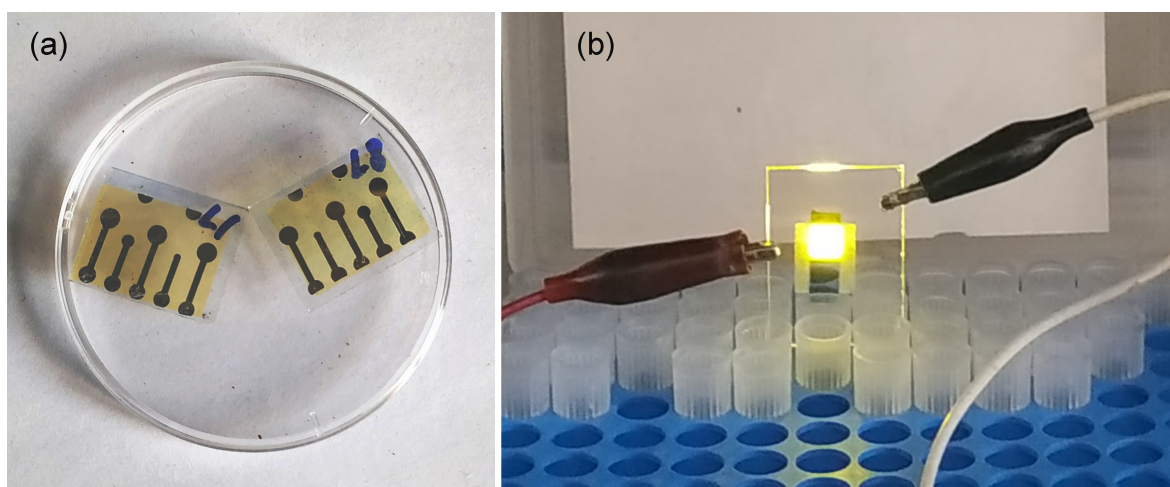
Figure 6. (a) Manufactured samples for the measurement of the charge carrier mobility by photo-MIS-CELIV method - glass/ITO/ SiO$_2$(70 nm)/ **1d**, **1h**, **1m**, or **2l** (100 nm)/Al (100 nm); (b) working OLED structure - ITO/ TAPC (80 nm) / **1m** (10 nm)/ 3TRYMB (30nm)/ LiF (1nm)/ Al (100 nm) (15B).
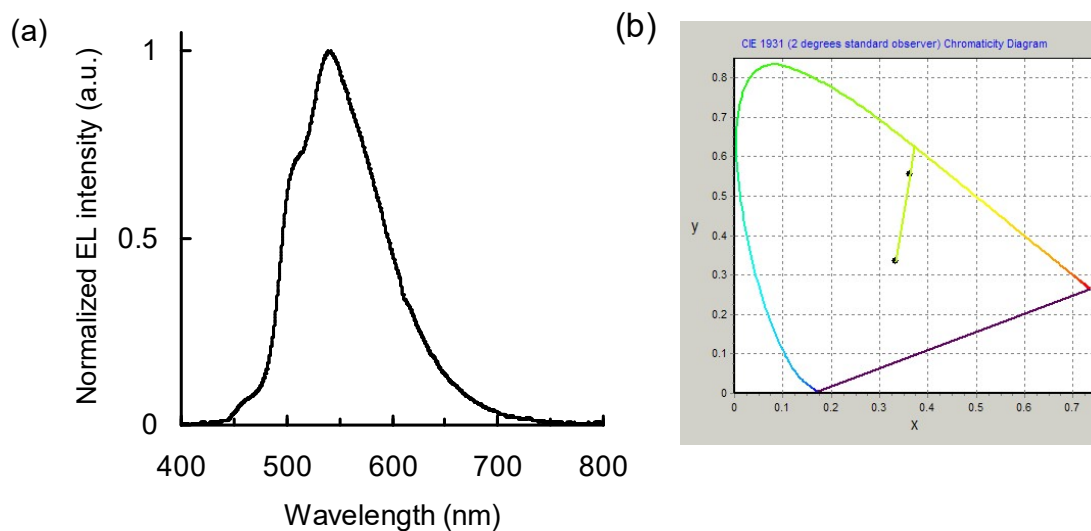
Figure 7. (a) Electroluminescence (EL) spectrum, (b) CIE chromaticity diagram (x = 0.363, y = 0.556) of OLED structure with **1m** as an emissive layer.

16
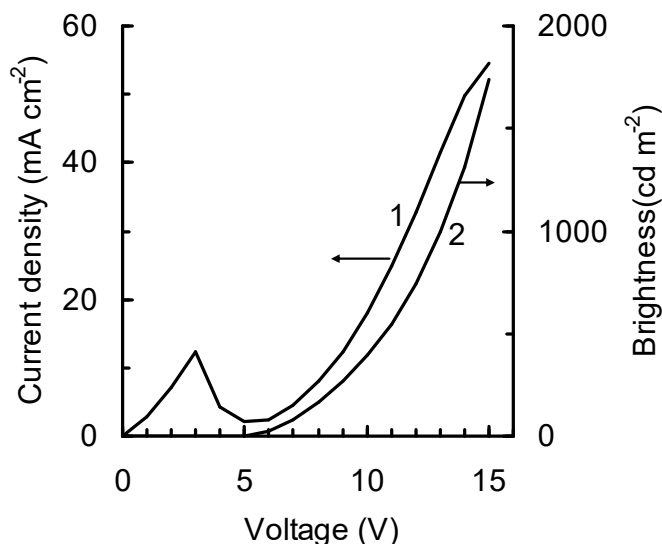
Figure 8. Voltage-current density (*1*) and voltage-brightness (*2*) characteristics of OLED with **1m** as an emissive layer.

Conclusions

In summary, we have shown that the selectivity of the rhodium-catalyzed oxidative coupling of aromatic carboxylic acids with internal alkynes strongly depends on the methylation of the supporting cyclopentadienyl ligand. This step- and atom economic approach provides access to isocoumarins using [Cp*RhCl$_2$]$_2$ as a catalyst and naphthalene derivatives in the case of [CpRhI$_2$]$_n$. The method is suitable for polyaromatic carboxylic acids to give π-extended isocoumarins and PAHs. The products show rich optical properties, with fluorescent efficiency being higher for PAHs. We have demonstrated their applicability as an emissive layer in OLED manufacturing.

Experimental Section

General: Catalytic reactions were carried out under an argon atmosphere in anhydrous *o*-xylene. Isolation of all products was carried out in air. Column chromatography was carried out using Macherey-Nagel silica gel 60 (0.04−0.063 mm particle size). Catalysts [Cp*RhCl$_2$]$_2$[19] and [CpRhI$_2$]$_n$[18a] were prepared as described in the literature. All other reagents were purchased from Acros or Aldrich and used as received. ^{1}H and ^{13}C{^{1}H} NMR spectra were recorded in CDCl$_3$ on a Varian Inova 400 spectrometer operating at 400.13 and 100.61 MHz, respectively. Chemical shifts are reported in ppm using the residual signals of the solvent as internal

17

standards. Electron impact mass spectra (EIMS) were recorded on a Kratos MS 890 instrument. Thermogravimetric analysis spectrum for **1m** was recorded on a Derivatograph-C instrument.

General procedure for the oxidative coupling of carboxylic acids with internal alkynes catalyzed by (cyclopentadienyl)rhodium complexes: A mixture of carboxylic acid (0.5 mmol), alkyne (1.0 mmol), [Cp*RhCl$_2$]$_2$ or [CpRhI$_2$]$_n$ (1 mol% Rh), Cu(OAc)$_2$·2H$_2$O (436 mg, 2.00 mmol) and *o*-xylene (2 ml) was refluxed with vigorous stirring for 6 h. The precipitate of copper salts was centrifuged off. The solvent was removed in vacuo and the residue was chromatographed on a silica column (1 × 15 cm). The first colorless band containing unreacted alkyne was eluted with petroleum ether. The second colored band was eluted with a mixture of petroleum ether and dichloromethane or ethyl acetate. Evaporation of the solvent gives a product, derivative of isocoumarin or naphthalene, respectively, as a colorless or yellow solid (or oil). Yields are given in Table 1.

3,4-Diphenyl-1H-isochromen-1-one (1a): colorless solid; SiO$_2$, petroleum ether/ dichloromethane (2:1); ^{1}H NMR (CDCl$_3$): δ = 7.20−7.45 (m, 12H), 7.55 (m, 1H), 7.66 (m, 1H), 8.44 (d, 1H, J = 8.0 Hz) ppm (cf.[13a]).

3,4-Bis(4-methoxyphenyl)-1H-isochromen-1-one (1b): yellow solid; SiO$_2$, petroleum ether/ ethyl acetate (10:1); ^{1}H NMR (CDCl$_3$): δ = 3.79 (s, 3H, OMe), 3.89 (s, 3H, OMe), 6.75 (d, 2H, J = 8.8 Hz), 6.99 (d, 2H, J = 8.4 Hz), 7.19 (d, 2H, J = 8.4 Hz), 7.22 (d, 1H, J = 7.6 Hz), 7.32 (d, 2H, J = 8.8 Hz), 7.50 (m, 1H), 7.64 (m, 1H), 8.40 (d, 1H, J = 7.8 Hz) ppm; ^{13}C NMR (CDCl$_3$): δ = 55.22 (OMe), 55.30 (OMe), 113.33 (2C), 114.61 (2C), 115.35, 120.20, 125.17, 125.45, 126.60, 127.66, 129.46, 130.64 (2C), 132.34 (2C), 134.55, 139.49, 150.88, 159.31, 159.87, 162.45 ppm; MS (EI-MS): calcd. for C$_{23}$H$_{18}$O$_4$ [M]$^+$ 358.1, found 358.1.

3,4-Diethyl-1H-isochromen-1-one (1c): orange oil; SiO$_2$, petroleum ether/ ethyl acetate (50:1); ^{1}H NMR (CDCl$_3$): δ = 1.19 (t, 3H, J = 7.7 Hz), 1.27 (t, 3H, J = 7.7 Hz), 2.58−2.67 (m, 4H), 7.44 (t, 1H, J = 8.2 Hz), 7.53 (d, 1H, J = 8.2 Hz), 7.72 (t, 1H, J = 8.2 Hz), 8.30 (d, 1H, J = 8.2 Hz) ppm; ^{13}C NMR (CDCl$_3$): δ = 12.53 (Et), 14.28 (Et), 19.28 (Et), 24.04 (Et), 113.04, 120.83, 122.43, 127.03, 129.83, 134.56, 137.72, 154.94, 162.96 ppm; MS (EI-MS): calcd. for C$_{13}$H$_{14}$O$_2$ [M]$^+$ 202.1, found 202.1.

6-Chloro-3,4-diphenyl-1H-isochromen-1-one (1d): colorless solid; SiO$_2$, petroleum ether/ dichloromethane (2:1); ^{1}H NMR (CDCl$_3$): δ = 7.12−7.27 (m, 6H), 7.34 (m, 2H), 7.40−7.54 (m, 4H), 8.34 (d, 1H, J = 8.4 Hz) ppm (cf.[13a]).

6-Methoxy-3,4-diphenyl-1H-isochromen-1-one (1e): colorless solid; SiO$_2$, petroleum ether/ dichloromethane (2:1); ^{1}H NMR (CDCl$_3$): δ = 3.72 (s, 3H, OMe), 6.55 (d, 1H, J = 2.4 Hz), 7.03 (dd, 1H, J = 8.8, 2.4 Hz), 7.10−7.44 (m, 10H), 8.31 (d, 1H, J = 8.8 Hz) ppm (cf.[25]).

18

3,4-Diphenyl-1H-benzo[h]isochromen-1-one (1h): colorless solid; SiO$_2$, petroleum ether/ dichloromethane (2:1); ^{1}H NMR (CDCl$_3$): δ = 7.01−7.58 (m, 11H), 7.65 (t, 1H, J = 7.6 Hz), 7.81 (t, 1H, J = 7.6 Hz), 7.89 (d, 1H, J = 8.0 Hz), 8.01 (d, 1H, J = 8.8 Hz), 9.89 (d, 1H, J = 8.4 Hz) ppm (cf.[25]).

3,4-Diphenylindeno[1,2-*h*]isochromen-1(11*H*)-one (1i): colorless solid; SiO$_2$, petroleum ether/ dichloromethane (1:1); ^{1}H NMR (CDCl$_3$): δ = 4.53 (s, 2H, CH$_2$), 7.12−7.60 (m, 13H), 7.71 (d, 1H, J = 6.4 Hz), 7.83 (d, 1H, J = 7.6 Hz), 8.04 (d, 1H, J = 8.4 Hz) ppm; ^{13}C NMR (CDCl$_3$): δ = 39.33 (CH$_2$), 117.27, 117.48, 119.87, 124.80, 125.19, 125.69, 126.85, 127.59, 127.86 (2C), 128.10, 128.79, 129.09 (2C), 129.22 (2C), 131.35 (2C), 133.13, 134.96, 138.00, 139.87, 142.43, 144.43, 146.30, 150.26, 161.60 ppm; MS (EI-MS): calcd. for C$_{28}$H$_{18}$O$_2$ [M]$^+$ 386.1, found 386.4; Anal. Calc. for C$_{28}$H$_{18}$O$_2$ (%): C, 87.02; H, 4.69. Found: C, 86.60; H, 4.96.

3,4-Diethylindeno[1,2-*h*]isochromen-1(11*H*)-one (1k): yellow solid; SiO$_2$, petroleum ether/ ethyl acetate (5:1); ^{1}H NMR (CDCl$_3$): δ = 1.27 (t, 3H, J = 7.5 Hz), 1.34 (t, 3H, J = 7.5 Hz), 2.65−2.76 (m, 4H), 4.46 (s, 2H, CH$_2$), 7.37−7.46 (m, 2H), 7.63 (d, 1H, J = 8.3 Hz), 7.68 (d, 1H, J = 8.3 Hz), 7.85 (d, 1H, J = 8.3 Hz), 8.16 (d, 1H, J = 8.3 Hz) ppm; ^{13}C NMR (CDCl$_3$): δ = 12.65 (Et), 14.35 (Et), 19.78 (Et), 24.14 (Et), 39.40 (CH$_2$), 113.47, 119.60, 121.61, 125.10, 125.75, 126.72, 127.25, 136.88, 139.98, 141.34, 144.24, 146.64, 152.96, 154.40, 162.29 ppm; MS (EI-MS): calcd. for C$_{20}$H$_{18}$O$_2$ [M]$^+$ 290.1, found 290.0.

7,8-Diphenyl-10H-phenaleno[1,9-gh]isochromen-10-one (1m): yellow solid; SiO$_2$, petroleum ether/ dichloromethane (1:1); ^{1}H NMR (CDCl$_3$): δ = 7.40−7.51 (m, 8H), 7.55−7.56 (m, 2H), 7.89−7.91 (m, 2H), 8.04−8.23 (m, 2H), 8.28 (d, 1H, J = 7.6 Hz), 8.40 (d, 1H, J = 7.6 Hz), 8.48 (d, 1H, J = 9.6 Hz), 10.24 (d, 1H, J = 9.6 Hz) ppm; ^{13}C NMR (CDCl$_3$): δ = 111.57, 117.29, 121.45, 123.60, 124.07, 125.87, 126.63, 126.95, 127.20, 127.42, 127.91 (2C), 128.24, 128.92, 129.26 (2C), 129.33 (2C), 130.38, 130.70, 130.97, 131.08, 131.74 (2C), 132.62, 133.12, 135.22, 135.90, 138.08, 150.91, 162.13 ppm; MS (EI-MS): calcd. for C$_{31}$H$_{18}$O$_2$ [M]$^+$ 422.1, found 422.0.

7,8-Bis(4-methoxyphenyl)-10H-phenaleno[1,9-gh]isochromen-10-one (1n): yellow solid; SiO$_2$, petroleum ether/ dichloromethane (1:2); ^{1}H NMR (CDCl$_3$): δ = 3.83 (s, 3H, OMe); 3.96 (s, 3H, OMe), 6.81 (d, 2H, J = 8.9 Hz), 7.10 (d, 2H, J = 8.9 Hz), 7.35 (d, 2H, J = 8.9 Hz), 7.44 (d, 2H, J = 8.9 Hz), 7.89−7.92 (m, 2H), 8.09−8.17 (m, 2H), 8.27 (d, 1H, J = 7.5 Hz), 8.39 (d, 1H, J = 7.7 Hz), 8.46 (d, 1H, J = 9.5 Hz), 10.23 (d, 1H, J = 9.5 Hz) ppm; ^{13}C NMR (CDCl$_3$): δ = 55.22 (OMe), 55.31 (OMe), 111.33, 113.35 (2C), 114.77 (2C), 115.69, 121.31, 123.62, 123.84, 125.38, 125.59, 125.84, 126.49, 126.81, 127.09, 127.43, 130.30, 130.64, 130.71 (2C), 130.81, 130.94, 132.55, 132.78 (2C), 135.83, 138.75, 150.83, 159.36, 159.83, 162.27 ppm; MS (EI-MS): calcd. for C$_{33}$H$_{22}$O$_4$ [M]$^+$ 482.2, found 482.2.

19

1,2,3,4-Tetraphenylnaphthalene (2a): yellow oil; SiO_2, petroleum ether/ ethyl acetate (10:1); ^{1}H NMR (CDCl₃): δ = 6.88−6.94 (m, 10H), 7.25−7.32 (m, 10H), 7.43−7.46 (m, 2H), 7.70−7.72 (m, 2H) ppm (cf.[13a]).

1,2,3,4-Tetrakis(4-methoxyphenyl)naphthalene (2b): brown solid; SiO_2, petroleum ether/ diethyl ether (3:1); ^{1}H NMR (CDCl₃): δ = 3.64 (s, 6H, OMe), 3.81 (s, 6H, OMe), 6.48 (d, 4H, J = 8.6 Hz), 6.76 (d, 4H, J = 8.6 Hz), 6.83 (d, 4H, J = 8.6 Hz), 7.13 (d, 4H, J = 8.6 Hz), 7.39−7.41 (m, 2H), 7.68−7.72 (m, 2H) ppm (cf.[13a]).

1,2,3,4-Tetraethylnaphthalene (2c): yellow oil; SiO_2, petroleum ether/ ethyl acetate (100:1); ^{1}H NMR (CDCl₃): δ = 1.34 (t, 3H, J = 7.5 Hz), 1.40 (t, 3H, J = 7.5 Hz), 2.93 (q, 2H, J = 7.5 Hz), 3.19 (q, 2H, J = 7.6 Hz), 7.47−7.51 (m, 2H); 8.09−8.13 (m, 2H) ppm (cf.[26]).

6-Chloro-1,2,3,4-tetraphenylnaphthalene (2d): yellow solid; SiO_2, petroleum ether/ dichloromethane (6:1); ^{1}H NMR (CDCl₃): δ = 6.88−6.91 (m, 10H), 7.22−7.28 (m, 10H), 7.57 (d, 1H, J = 8.0 Hz), 7.65 (d, 1H, J = 8.0 Hz), 7.68 (s, 1H) ppm (cf.[13a]).

6-Methoxy-1,2,3,4-tetraphenylnaphthalene (2e): yellow solid; SiO_2, petroleum ether/ dichloromethane (10:1); ^{1}H NMR (CDCl₃): δ = 3.75 (s, 3H, OMe), 6.90−6.95 (m, 10H), 7.05 (s, 1H), 7.15 (d, 1H, J = 9.1 Hz), 7.29−7.34 (m, 10H), 7.67 (d, 1H, J = 9.1 Hz) ppm (cf.[27]).

6-Methoxy-1,4-dimethyl-2,3-diphenylnaphthalene (2f): yellow solid; SiO_2, petroleum ether/ dichloromethane (3:1); ^{1}H NMR (CDCl₃): δ = 2.43 (s, 3H, Me), 2.45 (s, 3H, Me), 4.02 (s, 3H, OMe), 6.99−7.02 (m, 6H), 7.15−7.17 (m, 4H), 7.30 (dd, 1H, J = 9.2, 2.7 Hz), 7.43 (d, 1H, J = 2.7 Hz), 8.11 (d, 1H, J = 9.2 Hz) ppm; ^{13}C NMR (CDCl₃): δ = 16.96 (Me), 17.10 (Me), 55.39 (OMe), 104.02, 117.70, 125.81, 125.87, 126.82, 127.28 (2C), 127.29 (2C), 129.43, 129.47, 129.72, 130.45 (2C), 130.68 (2C), 133.36, 137.42, 140.07, 141.86, 142.00, 157.72 ppm; MS (EI-MS): calcd. for $C_{25}H_{22}O$ [M]$^+$ 338.2, found 338.2.

6-Nitro-1,2,3,4-tetraphenylnaphthalene (2g): yellow solid; SiO_2, dichloromethane; ^{1}H NMR (CDCl₃): δ = 6.90−6.94 (m, 10H), 7.24−7.35 (m, 10H), 7.84 (d, 1H, J = 9.4 Hz), 8.17 (dd, 1H, J = 9.4, 2.4 Hz), 8.69 (d, 1H, J = 2.4 Hz) ppm (cf.[27]).

1,2,3,4-Tetraphenyl-11*H*-benzo[*a*]fluorene (2i): yellow solid; SiO_2, dichloromethane; ^{1}H NMR (CDCl₃): δ = 3.28 (s, 2H, CH₂), 6.84−6.90 (m, 10H), 7.22−7.38 (m, 13H), 7.78 (d, 1H, J = 8.7 Hz), 7.81 (d, 1H, J = 7.5 Hz), 7.90 (d, 1H, J = 8.7 Hz) ppm; ^{13}C NMR (CDCl₃): δ = 39.31 (CH₂), 118.72, 119.30, 124.18, 125.20, 125.23, 126.22, 126.32 (2C), 126.39, 126.49 (2C), 126.55, 126.85, 127.52 (2C), 127.61 (2C), 127.71, 127.88, 131.22 (2C), 131.27 (2C), 131.36 (2C), 131.40 (2C), 132.16, 137.48, 138.23, 139.47, 139.98, 140.25, 140.38, 140.43, 140.56, 140.59, 141.11, 141.86, 144.24 ppm; MS (EI-MS): calcd. for $C_{41}H_{28}$ [M]$^+$ 520.2, found 519.9.

1,4-Dimethyl-2,3-diphenyl-11*H*-benzo[*a*]fluorene (2j): yellow solid; SiO_2, petroleum ether/ ethyl acetate (8:1); ^{1}H NMR (CDCl₃): δ = 2.56 (s, 3H, Me), 2.74 (s, 3H, Me), 4.59 (s, 2H, CH₂),

20

7.05−7.09 (m, 4H), 7.16−7.24 (m, 6H), 7.43 (t, 1H, J = 7.4), 7.53 (t, 1H, J = 7.4 Hz), 7.71 (d, 1H, J = 7.4 Hz), 7.98 (d, 1H, J = 7.4 Hz), 8.11 (d, 1H, J = 8.7 Hz), 8.29 (d, 1H, J = 8.7 Hz) ppm; ^{13}C NMR (CDCl$_3$): δ = 17.96 (Me), 21.15 (Me), 41.98 (CH$_2$), 118.71, 119.45, 124.29, 125.26, 125.82, 125.87, 126.26, 126.71, 127.25 (2C), 127.40 (2C), 130.13, 130.29, 130.43 (2C), 130.46 (2C), 131.21, 132.60, 139.00, 139.93, 139.95, 140.88, 141.41, 141.97, 142.18, 143.81 ppm; MS (EI-MS): calcd. for C$_{31}$H$_{24}$ [M]$^+$ 396.2, found 396.5.

1,2,3,4-Tetraphenylbenzo[*b*]naphtho[2,1-*d*]furan (2l): colorless solid; SiO$_2$, petroleum ether/ dichloromethane (2:1); ^{1}H NMR (CDCl$_3$): δ = 6.79−7.01 (m, 10H), 7.06−7.18 (m, 1H), 7.19−7.44 (m, 12H), 7.60−7.69 (m, 1H), 7.91−8.02 (m, 2H) ppm; ^{13}C NMR (CDCl$_3$): δ = 111.67, 118.55, 120.00, 120.32, 120.54, 122.59, 122.90, 124.06, 125.40 (2C), 126.00, 126.22, 126.49 (2C), 126.56, 126.59 (2C), 126.90 (2C), 127.61 (2C), 130.98 (2C), 131.29 (2C), 131.25 (2C), 131.40 (2C), 132.12, 135.42, 139.03, 139.26, 140.05, 140.08, 140.34, 140.50, 141.21, 152.43, 155.52 ppm; MS (EI-MS): calcd. for C$_{40}$H$_{26}$O [M]$^+$ 522.2, found 522.3.

7,8,9,10-Tetraphenylbenzo[*pqr*]tetraphene (2m): yellow solid; SiO$_2$, dichloromethane; ^{1}H NMR (CDCl$_3$): δ = 6.85−6.94 (m, 10H), 7.22−7.27 (m, 6H), 7.34−7.35 (m, 4H), 7.70 (d, 1H, J = 9.5 Hz,), 7.84 (m, 2H), 7.90−8.00 (m, 2H), 8.05 (m, 2H), 8.30 (s, 1H) ppm; ^{13}C NMR (CDCl$_3$): δ = 124.49, 124.53, 124.84, 124.99, 125.15, 125.19, 125.36, 126.17, 126.38, 126.50 (2C), 126.59 (2C), 126.63, 126.91, 127.65, 127.69 (2C), 127.75, 128.19, 128.31 (2C), 128.49, 129.84, 130.68, 131.08, 131.22 (2C), 131.47 (2C), 131.59 (2C), 131.74 (2C), 137.88, 138.92, 139.14, 140.24, 140.27, 140.73, 140.87, 143.66 ppm; MS (EI-MS): calcd. for C$_{44}$H$_{28}$ [M]$^+$ 556.2, found 556.9; Anal. Calc. for C$_{44}$H$_{28}$·CH$_2$Cl$_2$ (%): C, 84.23; H, 4.72. Found: C, 84.06; H, 4.86.

7,10-Dimethyl-8,9-diphenylbenzo[*pqr*]tetraphene (2o): yellow solid; SiO$_2$, petroleum ether/ dichloromethane (6:1); ^{1}H NMR (CDCl$_3$): δ = 2.79 (s, 3H, Me), 2.96 (s, 3H, Me), 7.12−7.24 (m, 10H), 7.96−8.04 (m, 2H); 8.08−8.13 (m, 2H), 8.26 (d, 2H, J = 8.9 Hz), 8.81 (s, 1H), 9.17 (d, 1H, J = 9.4 Hz) ppm; ^{13}C NMR (CDCl$_3$): δ = 17.91(Me), 25.46 (Me), 121.99, 124.61, 124.76, 125.12, 125.15, 125.95, 126.04, 126.08, 127.26 (2C), 127.56 (2C), 127.64, 127.67, 128.26, 128.47, 128.57, 128.93, 129.56 (2C), 129.64, 129.67, 130.25, 130.66 (2C), 130.68 (2C), 130.79, 130.82, 131.81, 139.34, 141.64, 141.92, 142.35 ppm; MS (EI-MS): calcd. for C$_{34}$H$_{24}$ [M]$^+$ 432.2, found 432.2.

7,8,9,10-Tetraethylbenzo[*pqr*]tetraphene (2p): brown solid; SiO$_2$, petroleum ether/ ethyl acetate (5:1); ^{1}H NMR (CDCl$_3$): δ = 1.38 (m, 6H), 1.56 (td, 3H, J = 7.6, 2.7 Hz), 1.80 (td, 3H, J = 7.3, 2.5 Hz), 3.10 (qd, 2H, J = 7.5, 2.7 Hz), 3.19 (qd, 2H, J = 7.4, 2.3 Hz), 3.44 (qd, 2H, J = 7.6, 2.5 Hz), 3.59 (bs, 2H), 7.89 (dd, 1H, J = 9.1, 1.8 Hz), 7.95−8.07 (m, 3H), 8.21 (dd, 2H, J = 9.4, 2.1 Hz), 8.73 (d, 1H, J = 2.4 Hz), 9.08 (dd, 1H, J = 9.4, 2.4 Hz) ppm; ^{13}C NMR (CDCl$_3$): δ = 16.08, 16.12, 16.20, 16.74, 22.66, 22.92, 23.01, 25.98, 121.79, 124.25, 124.29, 124.77, 124.82,

125.39, 125.83, 127.09, 127.21, 127.65, 128.57, 128.65, 128.68, 129.70, 130.80, 131.95, 135.79, 136.02, 138.28, 140.72 ppm; MS (EI-MS): calcd. for $C_{28}H_{28}$ [M]$^+$ 364.2, found 364.0.

General procedure for the oxidative coupling of carboxylic acids with internal alkynes catalyzed by mixture Cp*H/RhCl$_3$: A mixture of carboxylic acid (0.5 mmol), alkyne (1.1 mmol), Cp*H (10 μl, 0.06 mmol), RhCl$_3$ (2.1 mg, 0.01 mmol), Cu(OAc)$_2$·2H$_2$O (436 mg, 2.00 mmol) and *o*-xylene (2 ml) was refluxed with vigorous stirring for 6 h. Isolation and purification of products were carried out as described above.

Absorption and fluorescence spectroscopy: Absorption spectra were recorded on an Agilent Cary 300 double-beam UV-vis spectrophotometer in a standard 1 cm quartz cell (Helma QS with PTFE stopper). Fluorescence spectra were recorded on a FluoroLog-3-221 spectrofluorimeter at 20±1°C in a standard 1cm quartz cell. The observed fluorescence was detected at a direct angle relative to the excitation beam. The fluorescence spectra were corrected for the nonuniformity of detector spectral sensitivity and were normalized by the excitation light intensity, derived from calibrated built-in reference sensor values.

The fluorescence quantum yield of the sample was determined at 20±1 °C in CH$_3$CN solutions compared to quinine sulfate in 0.5M H$_2$SO$_4$ water solution as a standard (φ=0.55±0.03).[28] The quantum yield was calculated from the equation:[29]

$$\phi_i = \frac{S_i}{S_0} \times \frac{\phi_0(1-10^{-D_0})}{(1-10^{-D_i})} \times \frac{n_i^2}{n_0^2}$$

where φ_i and φ_0 are the quantum yields of the test solution and the standard; D_i and D_0 are the absorptions of the test solution and the standard, S_i and S_0 are the areas underneath corrected fluorescence spectrum curves for the test solution and the standard, n_i and n_0 are the refraction factors of the solvents of the test compound and the standard compound, respectively.

The luminescence quantum yield measurement for **1m** in the solid state was performed using of a HORIBA Jobin Yvon integration sphere (Model F-3018) at 298 K. All data were collected and processed using the Microsoft Excel software package (PLQY calculator v. 1.2.).

The fluorescence lifetime measurement for **1m** in acetonitrile solution was carried out using the time-correlated single-photon counting method realized on Fluorolog-3-221 spectrofluorimeter equipped with 340 nm NanoLED laser-diode source for fluorescence excitation. To fit fluorescence decay data and to determine fluorescence lifetime DataStation software (**DAS6**) was used.

The fluorescence spectra were normalized by the excitation light intensity, derived from the calibrated built-in reference sensor values. This normalization by the excitation light intensity

22

(as shown by the results of our tests) makes the integral intensity invariant to the changing the excitation slit width in the range from two to four times. If the slit width is varied more than four times, a negligible difference occurs between spectra intensity, so we limit slit width change by four times. The best effect of this normalization (when the normalized intensity does not depend on the slit change) occurs when the excitation wavelength corresponds to a flat area of the absorption spectra with a minimal optical density change upon wavelength (but not at an abrupt slope). This technique makes possible to measure the quantum yields of low-fluorescent probes by means of high-fluorescent standards with the excitation slit variation.

Spectroscopic grade acetonitrile (HPLC-S, Biosolve, #01200702) and CH_2Cl_2 (HPLC-grade, TU 6-09-2662-77) were used without further purification for solution preparation and recording of the absorption and fluorescence spectra. The concentrated solutions (MeCN and CH_2Cl_2) were prepared and stored in glass vials sealed with PTFE-shielded septa caps.

Solutions preparation: We encountered some experimental difficulties while investigating the optical properties since the compounds studied have limited solubility in CH_3CN, but have good solubility in CH_2Cl_2. CH_3CN as a solvent is convenient for the experiment: it is optically transparent over a wide UV-VIS range and its boiling point is not very low (this is essential for dosing units, that are used for dilution). CH_2Cl_2 has limited transparency in the UV range, so some bands of substances will be cropped by the solvent absorption. We decide to measure the absorption and emission spectra by diluting highly concentrated CH_2Cl_2 solutions ($3 \cdot 10^{-3}$M) with CH_3CN. Because of the low CH_2Cl_2 concentration we were not able to subtract its absorption from the UV spectrum with good accuracy. For compounds **1 m** and **2 m**, we demonstrated that the addition of CH_2Cl_2 to a CH_3CN solution does not affect the absorption and fluorescence spectra (for details, see the Supporting Information).

OLED manufacturing: The CELIV set-up included a digital USB-oscilloscope (DL-Analog Discovery, Digilent Co.), which played the role of a master pulse generator and a transient current pulse monitor. *RC* constants were at least a factor of 20 smaller than the time scales of interest. The bias was swept in the range between 10 and 100 kHz. The electroluminescence spectra of OLEDs were recorded on an Avantes 2048 fiber-optic spectrofluorimeter (spectral range 200–1100 nm, spectral resolution better than 0.04 nm). Voltage–current and voltage–brightness characteristics were measured with a Keithley 2601 SourceMeter, a Keithley 485 picoammeter and a TKA-04/3 luxmeter–brightness meter. The preparation of OLED samples and measurements of their spectral and optoelectronic characteristics were performed at room temperature under argon atmosphere with a controlled content of oxygen and water (below 1 ppm). The thickness of the films was determined using a LOMO MII-4 interferometer.

23

Supporting Information (see footnote on the first page of this article): Crystallographic data and copies of NMR, absorption and fluorescence spectra.

Keywords: C-H activation; fluorescence; organic light-emitting diode; polycycles; rhodium catalysis

24

Table of Contents entry

A short text

From catalysis to OLEDs: The selectivity of the rhodium-catalyzed oxidative coupling of carboxylic acids and internal alkynes strongly depends on the methylation of the Cp ligand at the rhodium atom. This approach provides easy access to isocoumarins and PAHs with extended π-conjugation for their further application as fluorescent materials. In particular, they exhibit fluorescence emission in the blue-green region (400–550 nm). Based on 7,8-diphenyl-10H-phenaleno[1,9-*gh*]isochromen-10-one as an emissive layer, the OLED structure was manufactured.

Graphical Element
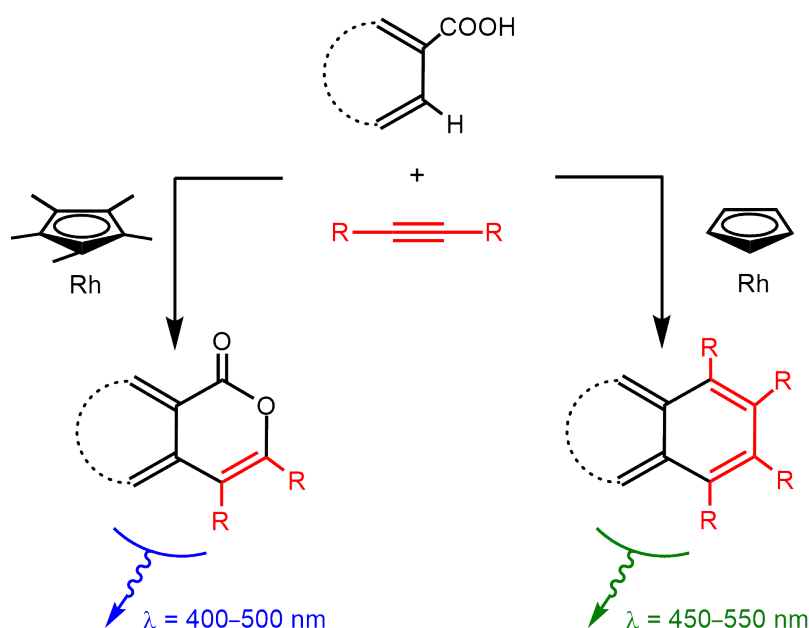
References

[1] For some recent works, see: a) A. Salehi, X. Fu, D.-H. Shin, F. So, *Adv. Funct. Mater.* **2019**, *29*, 1808803; b) Q. Wei, N. Fei, A. Islam, T. Lei, L. Hong, R. Peng, X. Fan, L. Chen, P. Gao, Z. Ge, *Adv. Optical Mater.* **2018**, *6*, 1800512; c) C. Bizzarri, E. Spuling, D. M. Knoll, D. Volz, S. Bräse, *Coord. Chem. Rev.* **2018**, *373*, 49–82; d) A. N. Aslandukov, V. V. Utochnikova, D. O.

Goriachiy, A. A. Vashchenko, D. M. Tsymbarenko, M. Hoffmann, M. Pietraszkiewicz, N. P. Kuzmina, *Dalton Trans.* **2018**, *47*, 16350–16357.

[2] C. W. Tang, S. A. VanSlyke, *Appl. Phys. Lett.* **1987**, *51*, 913–915.

[3] a) D. A. Loginov, A. P. Molotkov, N. E. Shepel, *J. Organomet. Chem.* **2018**, *867*, 67–70; b) S. Mayakrishnan, Y. Arun, N. U. Maheswari, P. T. Perumal, *Chem. Commun*. **2018**, *54*, 11889–11892; c) T. Han, H. Deng, C. Y. Y. Yu, C. Gui, Z. Song, R. T. K. Kwok, J. W. Y. Lam, B. Z. Tang, *Polym. Chem.* **2016**, *7*, 2501–2510; d) C. Kitamura, T. Ohara, A. Yoneda, T. Kawase, T. Kobayashi, H. Naito, *Chem. Lett*. **2011**, *40*, 58–59.

[4] a) Y. Li, T. Yu, W. Su, Y. Wang, Y. Zhao, H. Zhang, *Arab. J. Chem.*, doi: 10.1016/j.arabjc.2019.05.006; b) T. M. Figueira-Duarte, P. G. Del Rosso, R. Trattnig, S. Sax, E. J. W. List, K. Müllen, *Adv. Mater.* **2010**, *22*, 990–993; c) Y. Yamashita, *Sci. Technol. Adv. Mater.* **2009**, *10*, 024313; d) W. Sotoyama, H. Sato, M. Kinoshita, T. Takahashi, A. Matsuura, J. Kodama, N. Sawatari, H. Inoue, *SID Digest* **2003**, *45*, 1294–1297.

[5] a) P. Saikia, S. Gogoi, *Adv. Synth. Catal.* **2018**, *260*, 2063–2075, and references therein; b) R. C. Larock, M. J. Doty, X. Han, *J. Org. Chem.* **1999**, *64*, 8770–8779.

[6] a) K. Komeyama, T. Kashihara, K. Takaki, *Tetrahedron Lett.* **2013**, *54*, 5659–5662; b) W. Huang, X. Zhou, K. Kanno, T. Takahashi, *Org. Lett.* **2014**, *6*, 2429–2431; c) G. Wu, A. L. Rheingold, S. J. Geib, R. F. Heck, *Organometallics* **1987**, *6*, 1941–1946.

[7] a) W.-J. Kong, L. H. Finger, J. C. A. Oliveira, L. Ackermann, *Angew. Chem.* **2019**, *131*, 6408–6412; b) T. Fukutani, K. Hirano, T. Satoh, M. Miura, *J. Org. Chem.* **2011**, *76*, 2867–2874; c) T. Uto, M. Shimizu, K. Ueura, H. Tsurugi, T. Satoh, M. Miura, *J. Org. Chem.* **2008**, *73*, 298–300; d) T. Yasukawa, T. Satoh, M. Miura, M. Nomura, *J. Am. Chem. Soc.* **2002**, *124*, 12680–12681.

[8] a) J. Gao, S. Zhang, Y. Zhang, *Tetrahedron* **2018**, *74*, 6263–6269; b) N. Umeda, H. Tsurugi, T. Satoh, M. Miura, *Angew. Chem. Int. Ed.* **2008**, *47*, 4019–402.

[9] M. V. Pham, N. Cramer, *Angew. Chem. Int. Ed.* **2014**, *53*, 3484–3487.

[10] D. A. Loginov, V. E. Konoplev, *J. Organomet. Chem.* **2018**, *867*, 14–24.

[11] For C–H activation under chelation-assistance by carboxylic group, see: M. P. Drapeau, L. J. Goossen, *Chem. Eur. J.* **2016**, *22*, 18654–18677.

[12] T. Satoh, M. Miura, *Chem. Eur. J*. **2010**, *16*, 11212–11222.

[13] a) K. Ueura, T. Satoh, M. Miura, *J. Org. Chem.* **2007**, *72*, 5362–5367; b) M. Shimizu, K. Hirano, T. Satoh, M. Miura, *J. Org. Chem.* **2009**, *74*, 3478–3483.

[14] D. A. Loginov, A. O. Belova, A. R. Kudinov, *Russ. Chem. Bull*. **2014**, *63*, 983−986.

[15] a) Y. Honjo, Y. Shibata, E. Kudo, T. Namba, K. Masutomi, K. Tanaka, *Chem. Eur. J.* **2018**, *24*, 317–321; b) E. Kudo, Y. Shibata, M. Yamazaki, K. Masutomi, Y. Miyauchi, M. Fukui, H. Sugiyama, H. Uekusa, T. Satoh, M. Miura, K. Tanaka, *Chem. Eur. J.* **2016**, *22*, 14190–14194.

[16] a) H. Chen, L. Ouyang, J. Liu, W.-J. Shi, G. Chen, L. Zheng, *J. Org. Chem*. **2019**, *84*, 12755−12763; b) P. Sihag, M. Jeganmohan, *J. Org. Chem*. **2019**, *84*, 2699−2712; c) D. A. Loginov, L. S. Shul'pina, D. V. Muratov, G. B. Shul'pin, *Coord. Chem. Rev*. **2019**, *387*, 1–31; d) V. B. Kharitonov, D. V. Muratov, D. A. Loginov, *Coord. Chem. Rev.* **2019**, *399*, 213027; e) R. Mandal, B. Sundararaju, *Org. Lett.* **2017**, *19*, 2544−2547; f) D. A. Loginov, D. V. Muratov, Y. V. Nelyubina, J. Laskova, *J. Mol. Catal. A: Chemical* **2017**, *426*, 393–397; g) D. A. Loginov, A. O. Belova, A. V. Vologzhanina, A. R. Kudinov, *J. Organomet. Chem.* **2015**, *793*, 232–240; h) S. Warratz, C. Kornhaass, A. Cajaraville, B. Niepötter, D. Stalke, L. Ackermann, *Angew. Chem. Int. Ed.* **2015**, *54*, 5513–5517; i) D. A. Frasco, C. P. Lilly, P. D. Boyle, E. A. Ison, *ACS Catal.* **2013**, *3*, 2421−2429; j) L. Ackermann, J. Pospech, H. K. Potukuchi, *Org. Lett.* **2012**, *14*, 2146–2149.

[17] For some recent examples of the use of modified CpRh complexes for C–H activation, see: a) R. Yoshimura, Y. Shibata, T. Yamada, K. Tanaka, *J. Org. Chem.* **2019**, *84*, 2501−2511; b) M. Brauns, N. Cramer, *Angew. Chem. Int. Ed.* **2019**, *58*, 8902–8906; c) J. Terasawa, Y. Shibata, M. Fukui, K. Tanaka, *Molecules* **2019**, *23*, 3325; d) E. J. T. Phipps, T. Rovis, *J. Am. Chem. Soc.* **2019**, *141*, 6807–6811; e) R. Yoshimura, Y. Shibata, S. Yoshizaki, J. Terasawa, T. Yamada, K. Tanaka, *Asian J. Org. Chem*. **2019**, *8*, 986–993; f) S.-G. Wang, N. Cramer, *Angew. Chem. Int. Ed.* **2019**, *58*, 2514–2518; g) E. A. Trifonova, N. M. Ankudinov, M. V. Kozlov, M. Y. Sharipov, Y. V. Nelyubina, D. S. Perekalin, *Chem. Eur. J.* **2018**, *24*, 16570–16575.

[18] a) D. A. Loginov, M. M. Vinogradov, Z. A. Starikova, P. V. Petrovskii, A. R. Kudinov, *Russ. Chem. Bull.* **2004**, *53*, 1949−1953; b) W. Lin, W. Li, D. Lu, F. Su, T.-B. Wen, H.-J. Zhang, *ACS Catal.* **2018**, *8*, 8070−8076.

[19] C. White, A. Yates, P. M. Maitlis, *Inorg. Synth.* **1992**, *29*, 228–234.

[20] For the mechanism of oxidative coupling of benzoic acids with alkynes, see: a) V. P. Datsenko, Y. V. Nelyubina, A. F. Smol'yakov, D. A. Loginov, *J. Organomet. Chem*. **2018**, *874*, 7–12; b) I. Funes-Ardoiz, F. Maseras, *Angew. Chem., Int. Ed*. **2016**, *55*, 2764–2767.

[21] CCDC 1951996 (**1i**) and CCDC 1951997 (**2o**) the supplementary crystallographic data for this paper. These data can be obtained free of charge from The Cambridge Crystallographic Data Centre.

27

[22] For *in situ* application of cyclopentadienes in C–H activation, see: a) B. Audic, M. D. Wodrich, N. Cramer, *Chem. Sci.* **2019**, *10*, 781–787; b) D. L. Davies, C. E. Ellul, K. Singh, *J. Organomet. Chem.* **2019**, *879*, 151–157.

[23] For some selected works, see: a) D. Zych, A. Slodek, A. Frankowska, *Comput. Mater. Sci.* **2019**, *165*, 101–113; b) N. Gelfand, A. Freidzon, V. Vovna, *Spectrochim. Acta A Mol. Biomol. Spectrosc*. **2019**, *216*, 161–172; c) N. Jiwalak, R. Daengngern, T. Rungrotmongkol, S. Jungsuttiwong, S. Namuangruk, N. Kungwan, S. Dokmaisrijan, *J. Lumin*. **2018**, *204*, 568–572; d) P. Krawczyk, *J. Mol. Model*. **2015**, *21*, 118; e) D. Guillaumont, S. Nakamura, *Dyes and Pigments* **2000**, *46*, 85–92.

[24] Y. Gao, A. Pivrikas, B. Xu, Y. Liu, W. Xu, P. H. M. van Loosdrecht, W. Tian, *Synthetic Metals* **2015**, *203*, 187–191.

[25] R. K. Chinnagolla, M. Jeganmohan, *Chem. Commun.* **2012**, *48*, 2030–2032.

[26] J.-C. Hsieh, C.-H. Cheng, *Chem. Commun*. **2008**, 2992–2994.

[27] A. Bej, A. Chakraborty, A. Sarkar, *RSC Adv*. **2013**, *3*, 15812–15819.

[28] J. N. Demas, "Measurement of Photon Yields" Optical Radiation Measurements, vol. 3, Academic Press, 1982, p. 195.

[29] S.P. Nighswander-Rempel, J. Riesz, J. Gilmore, P. Meredith, *J. Chem. Phys.* **2005**, *123*, 194901.

28